Spectral Intensity Patterns and Vibrational Phase Space Structure†

Vivian Tyng and Michael E. Kellman*

91 Klamath Hall, Department of Chemistry, University of Oregon, Eugene, Oregon 97403-1253

Received: April 30, 2009

We examine patterns of absorption intensity in two-mode systems with a 2:1 Fermi resonance in an intensity model based on the effective fitting Hamiltonian. We relate these patterns to the Fermi resonance phase space structure and catastrophe map. Each of the four zones of the catastrophe map has a phase sphere structure with a certain number of distinct regions. For each zone, we find that for every region on the sphere, there is a distinct region in the intensity pattern.

I. Introduction

It is well established that nonlinear effects of anharmonicity and coupling of normal modes have a profound effect on molecular vibrational dynamics. An extended line of investigation employs ideas of classical phase space structure and bifurcations.[1−31] Experimental access to these phenomena has been achieved, relying mostly on energy-level patterns,[7] with use of effective spectroscopic fitting Hamiltonians to make the link between experiment and dynamics. In contrast, there has been far less systematic use of intensity patterns as a probe of phase space structure. This is a serious limitation because access to phase space structure and dynamics on the basis of energy-level patterns will very rapidly become more difficult as the number of coupled modes increases; this becomes starkly evident even with the stretch−bend dynamics of C_2H_2. In this paper, we attempt to begin to fill this gap, beginning with the simplest examples where there is some experimental evidence. We will use a simple model of Quack and co-workers[32−34] for experimental absorption intensities to investigate patterns in the spectra of systems with an anharmonic resonance, specifically the standard 2:1 Fermi resonance, relying on earlier systematic investigations[5,7] of phase space structure and energy-level patterns in resonant systems. We will concentrate on the highly excited C−H stretch−bend resonance in substituted methanes, a system that was extensively studied experimentally quite a while ago,[32−34] and also the CO_2 spectral fit.[35]

II. Resonances, Bifurcations, Catastrophe Map, and Energy-Level and Intensity Patterns

Our earlier work emphasized that anharmonic resonances lead to bifurcations in phase space in which new modes are born out of normal modes or even erupt "out of nothing". For a single resonance between two modes, the phase space structure is conveniently mapped on the polyad phase sphere,[3] a representation reduced in dimension by the presence of a polyad number, one sphere for each polyad. The structure of the spheres for a given form of the resonance Hamiltonian can be mapped onto the catastrophe map,[5,7,14,17] a kind of phase diagram. Each zone of the map corresponds to a distinct phase sphere structure. Distinct energy-level patterns are found for each zone.[7] The patterns consist of well-marked indicators of phase space separatrix structure when differences in energy of adjacent levels in phase space are plotted.

Our strategy for intensities is the following. In the 2:1 Fermi resonance system, the catastrophe map has four zones, corresponding to four types of phase space structure. In ref 7, we examined energy patterns of molecules with a 2:1 Fermi resonance between the local stretch and bend of a C−H group. One molecule that we examined was $HC(CF_3)_3$, with polyads in all four zones. We also looked at energy patterns for each of the four zones using several different substituted methanes as well as CO_2, choosing an example for each zone that brings out the pattern for that zone most clearly.

We follow a parallel path here, now relating intensity patterns as well as energy patterns to the catastrophe map. The four zones differ in the phase space structure at and surrounding the zero-order C−H local mode stretch overtone. The intensity model will be based on the supposition that dipole strength is carried by the C−H local mode stretch overtone, a not unreasonable first approximation. Intensity is then spread among the eigenstates because of mixing of zero-order states by the Fermi resonance coupling.

At the outset, we can frame a hypothesis concerning the intensity patterns based upon our earlier experience with energy patterns. We found in ref 7 that there were four zones I−IV on the catastrophe map. Each zone corresponds to a distinct phase sphere structure, including the structure surrounding the C−H stretch bright mode. For each phase sphere type, there is a definite number of distinct regions on the sphere. For zones I, II, III, and IV, the spheres have, respectively, 1, 2, 3, and 1 distinct regions. We found that in the energy-level spacing plots, there were as many regions as on the sphere. Thus, the zone III sphere with three phase space regions has three distinct regions in the energy spacing plots when properly analyzed; see Figure 8 of ref 7. We make a corresponding hypothesis regarding the intensities; for each phase space region on a sphere, there will be a distinct region in the intensity plot. Thus zones I, II, III, and IV would have, respectively, 1, 2, 3, and 1 intensity regions.

III. Fermi Resonance Model

We work with a model for the molecular Hamiltonian and a distinct model for calculating intensities with the help of this molecular Hamiltonian.

A. Effective Molecular Fitting Hamiltonian. The molecular Hamiltonian is standard and has been used[7] for analyzing the phase space structure of the 2:1 Fermi resonance. The two modes are taken to be anharmonic modes in an approximate 2:1 frequency ratio; we will take these to be a stretch s and bend b.

† Part of the "Robert W. Field Festschrift".

* To whom correspondence should be addressed.

10.1021/jp904038f CCC: $40.75
Published on Web 07/17/2009

The Hamiltonian has a zero-order part diagonal in the quantum numbers and a coupling term that exchanges two quanta of bend for one of stretch

$$\begin{aligned} H_{2:1} &= H_{02} + V_{2:1} \\ H_{02} &= (n_s + 1/2)\omega_s + (n_b + 1)\omega_b + X_{ss}(n_s + 1/2)^2 + \\ &\qquad X_{sb}(n_s + 1/2)(n_b + 1) + X_{bb}(n_b + 1)^2 \\ V_{2:1} &= \kappa_{sbb}(a_s^+ a_b a_b + a_s a_b^+ a_b^+)/\sqrt{2} \end{aligned} \tag{1}$$

It is easy to verify that the 2:1 coupling preserves as a polyad number the sum

$$n_{sb} = (n_s + n_b/2) \tag{2}$$

This Fermi resonance Hamiltonian has been systematically analyzed in ref 7 on the catastrophe map, a kind of "phase diagram" that exhaustively classifies the types of phase space structures possible given the form of the Hamiltonian. There are four zones in the catastrophe map. Given the parameters of the fit, the spectrum of a particular molecule can be plotted as a series of points on the map, each point representing a polyad.

B. Intensity Model. Our intensity model is intentionally a very simple "minimal" model, used by Quack and co-workers[32−34] to model experimental intensities in substituted methane spectra. A similar model was used by Field and co-workers[24] for intensities of highly excited bend states in acetylene, however in dispersed fluorescence rather than absorption spectra. We assume that all of the intensity is carried by the zero-order stretch overtone. Therefore, within a polyad, the relative intensity of each eigenstate is given by the fraction of zero-order stretch in the eigenstate. In terms of zero-order states $|n_s,n_b\rangle$ the ground state is $|\mathbf{0}\rangle = |0,0\rangle$, and the α eigenstate of the ν polyad is

$$|\Psi^{\alpha,\nu}\rangle = \sum_{n_s,n_b} c^{\nu,\alpha}_{n_s,n_b} |n_s, n_b\rangle \tag{3}$$

Then, the transition matrix element for states in the ν polyad is

$$\langle \Psi^{\nu,\alpha}|\mu|\mathbf{0}\rangle = \sum_{n_s,n_b} c^{\nu,\alpha}_{n_s,n_b} \langle n_s, n_b|\mu|0, 0\rangle \tag{4}$$

$$= c^{\nu,\alpha}_{\nu,0} \langle \nu, 0|\mu|0, 0\rangle \tag{5}$$

$$= c^{\nu,\alpha}_{\nu,0} \langle \nu|\mu|0\rangle \tag{6}$$

$$= c^{\nu,\alpha}_{\nu,0} M_\nu \tag{7}$$

and the intensity is

$$I_{\nu,\alpha} = |\langle \Psi^{\nu,\alpha}|\mu|\mathbf{0}\rangle|^2 = |c^{\nu,\alpha}_{\nu,0} M_\nu|^2 \tag{8}$$

Thus, since all of the intensity in the ν polyad is carried by the zero-order overtone state $|\nu,0\rangle$, the intensity of the α eigenstate of the ν polyad (relative to intensity 1 for the zero-order overtone state) is $|c^{\nu,\alpha}_{\nu,0}|^2$

This intensity model was used by Quack and co-workers[32−34] to analyze experimental spectra of highly excited C−H stretch−bend Fermi resonance systems in substituted methanes, with good agreement for the first few polyads.

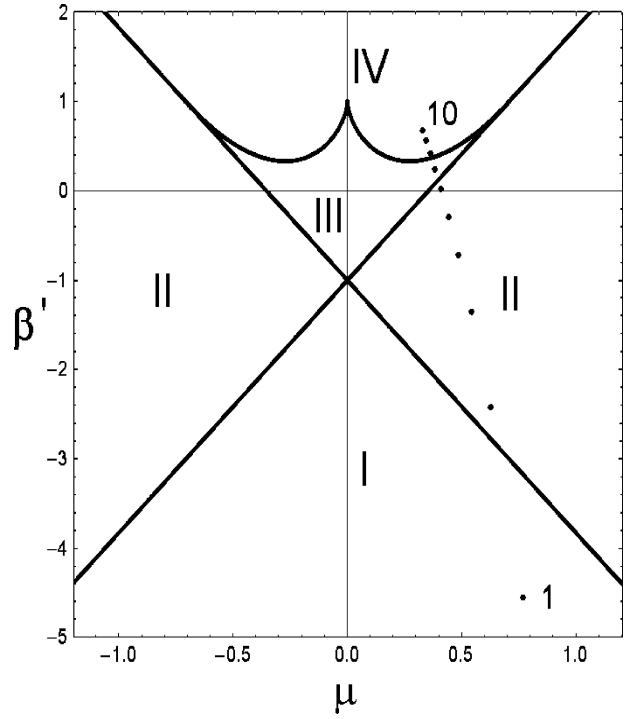

Figure 1. Catastrophe map for the 2:1 Fermi resonance, with polyads $P = 1-10$ of $HC(CF_3)_3$. The map with its structure of zones I−IV and control parameters μ,β' is described in ref 5.

IV. Intensity Results and Patterns

A. $HC(CF_3)_3$. We first consider $HC(CF_3)_3$ as case of a molecule whose polyads traverse all four zones of the catastrophe map. Figure 1 shows the polyads of $HC(CF_3)_3$ on the map. Their placement is polyad 1 in zone I, polyads 2−6 in zone II, polyad 7 in zone III, and polyads 8−10 in zone IV. The intensities are shown in Figure 2, with both logarithmic and linear scales. Each polyad is normalized to unit total intensity. The goal is to analyze relative intensities within polyads; the actual experimental intensity falls off sharply with polyad number. The match of the relative intensities in the model to experiment was considered in refs 32−34. There was fair agreement, deteriorating at the highest observed polyads, which went up to polyad 6. Here, we extrapolate the intensity model to higher polyads in order to see how the pattern in the model changes as all of the zones of the catastrophe map are accessed.

Several distinct patterns are visible. The spectrum starts off with almost all of the intensity in the highest energy state at the right in polyads 1 and 2. Then, the intensity becomes widely distributed, with the most intense member in the middle in polyads 3−7. Finally, in polyads 8−10, the intensity is strongly concentrated in the single most intense member, isolated at low energy from other members of the polyad. Evidently, there is a pretty close correspondence between the intensity pattern of a given polyad and its location among the catastrophe map zones, though there is no clear differentiation between zones II and III. This will be clarified in the next section as being connected with the fact that both zones II and III are resonant zones, though with somewhat different phase space structure.

B. Representative Exemplars of the Zones. Next, as in ref 7, we consider stretch−bend polyads of several different molecules and relate their intensity and energy patterns to their

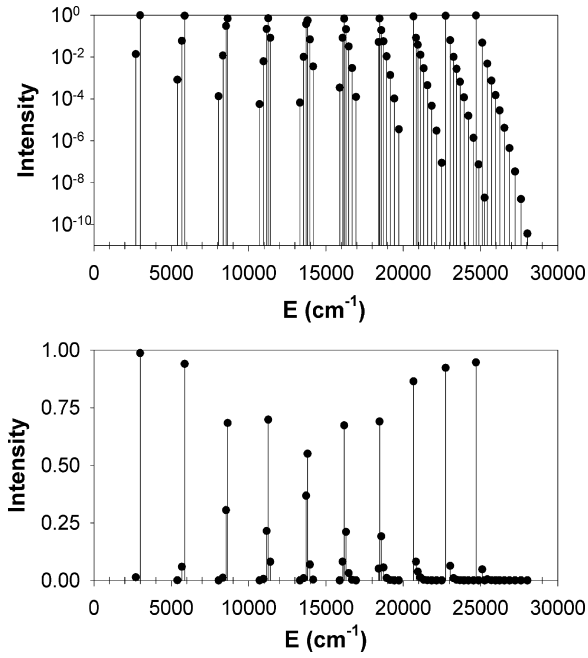

Figure 2. Model intensities for polyads $P = 1-10$ of $HC(CF_3)_3$. The upper plot is logarithmic and the lower plot linear.

location in each of the four catastrophe map zones, choosing examples that bring out the pattern for each zone most clearly. We will again consider coupled C−H stretch and bend in substituted methanes and also the CO_2 stretch−bend Fermi resonance system, the latter as an example of a nearly pure "fully bifurcated" zone II molecule, that is, with all polyads in zone II. We choose examples where the polyad number is $P = 10$ in order to have a lot of levels that clearly show the pattern. The polyads of molecules chosen as exemplars, their location in the catastrophe map, their polyad phase spheres, and their intensity and energy patterns are shown in Figure 3. The energy patterns are spacings between levels which semiclassically are adjacent in phase space; these were already discussed in great detail in ref 7, and they are repeated in Figure 3 for comparison with the intensity patterns.

As a general observation, note how in moving through zones I−IV, the level of maximum intensity, with a maximum fraction of the C−H stretch overtone, moves through the polyads, from right to middle to left, that is, from highest-energy to lowest-energy member of the polyad. This pattern was already seen for the previously considered $HC(CF_3)_3$.

Case I is an artificial molecule with $P = 10$ zone I (it is hard to find a resonant molecule that stays in zone I, that is, out of resonance for such a high polyad number) with the level

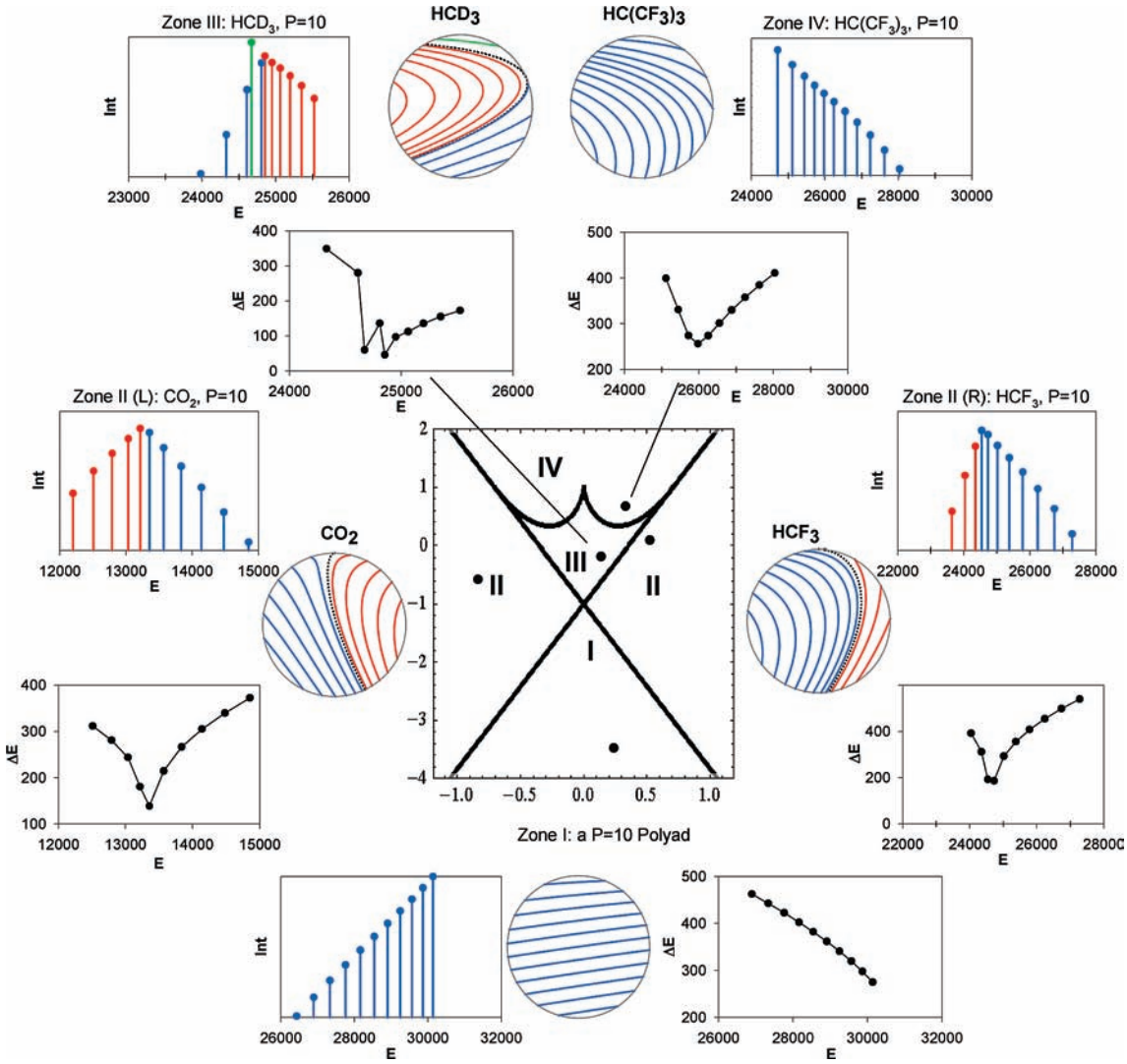

Figure 3. Zone classification, polyad phase spheres (described in text), intensity patterns, and energy spacing patterns for $P = 10$ polyads of selected molecules.

conventionally assigned as the C−H stretch mode overtone as the high-energy member of polyad. There is an undivided polyad phase sphere, without a separatrix. The C−H stretch mode is a stable mode represented by an elliptic fixed point exactly at the north pole because of molecular symmetry. The intensities change monotonically with energy, in perfect accord with the fraction of the zero-order C−H stretch in the series of trajectories descending from the north pole, corresponding to the quantum levels, and also in accord with the undivided character of the phase sphere. This matches the pattern of monotonic energy spacings.

Case II is HCF_3 with $P = 10$ in zone II. The phase sphere is far different from that in zone I. Now, there is a separatrix which runs through the north pole, with an unstable cusp at the pole, corresponding to the pure C−H stretch. The separatrix divides the sphere into two regions, each surrounding a stable fixed point, corresponding to resonant collective modes.[2,3,5,6] The unstable C−H stretch is the intermediate energy member of polyad. The intensities decrease monotonically in both directions from the C−H stretch. This division of intensity perfectly reflects the unstable character of the C−H bright mode and the division of the phase sphere into two regions. The intensity pattern again matches the energy spacing pattern.

A second example of zone II is CO_2. We show this because CO_2 is an almost perfect example of a strongly resonant, "pure zone II" molecule. This is reflected in the division of the phase sphere and the intensity pattern.

Case III is HCD_3 with $P = 10$ in zone III. This is the most interesting of the four zones. On the catastrophe map, the polyads have moved out of the strongly resonant zone II. The phase sphere now has three regions, one surrounding the C−H stretch and the others surrounding resonant collective modes. On the sphere, the C−H stretch is again a stable fixed point like zone I, but now in a separate, isolated region. The concentration of intensity that is especially apparent in a linear rather than logarithmic plot reflects that the C−H bright mode is stable. Following our hypothesis, we expect that there should be three regions in the intensity plot, corresponding to these three phase sphere regions. This is brought out by the color coding of Figure 3, which separates the intensity into three regions and shows their correspondence with the regions of the sphere. The isolation of the bright mode reflects that it is in its own isolated stable region of phase sphere. The energy spacings have a "zigzag" pattern, as in the figure; the reason for this is the existence of three regions on the sphere. Reference 7 showed how the zigzag can be resolved into a smooth "fan" of energy spacings, as seen in Figure 8 of that paper.

Case IV is $HC(CF_3)_3$ with $P = 10$ in zone IV. The phase sphere is again nonresonant. This is like zone I, but in zone IV, the energy spacings show a minimum, something like a remnant of the separatrix structure of zones II and III. Note however that the intensity pattern for zone IV is monotonic, in contrast to the energy pattern and similar to the intensity pattern of zone I.

V. Conclusions

We have found that there are distinct intensity patterns associated with the changes in the phase space structure in our model of the 2:1 Fermi stretch−bend resonance. With the help of polyad phase spheres and their classification on the catastrophe map, we have gotten a rational account of the intensity pattern within a polyad. The pattern gives information about the phase space structure at and surrounding the bright state. As the polyad number changes, there are signatures of bifurcations in the phase space structure. The combination of energy and intensity patterns gives a way to "track" the spectrum as the polyads tune through the catastrophe map. A systematic rule relates the zones of the catastrophe map to the intensity patterns. Each zone I−IV has phase spheres with a certain number of distinct regions on the sphere; we have found in the intensity plots that within each zone, there is a distinct region in the intensity pattern corresponding to each phase sphere region. This parallels the finding in ref 7 of a distinct region in the energy-level pattern for each phase sphere region. Thus, there is a one-to-one correspondence between regions of the phase sphere, regions of the intensity pattern, and regions of the energy-level pattern.

From a more general point of view, the present work is a beginning in the use of intensity patterns to detect changes in phase space structure and dynamics in highly anharmonic systems with many quanta. For the simple two-mode single-resonance systems considered here, the dynamical changes are relatively easy to determine from the energy-level patterns alone. However, in systems with many modes and resonance couplings, the detection of changes in dynamics due to bifurcations through assignment of energy patterns can become very complex. Intensity patterns are probably more directly observable, and it is critical to be able to use their measurement as a probe of the evolving phase space. We plan to use extensions of the ideas in this paper to build intensity models for more complex systems, such as the three-mode H_2O system and larger systems such as C_2H_2. It must be said that this will be a much greater challenge than what we have done here. Apart from the much greater complexity of systems with more than two modes, the "minimal" intensity model used here will almost surely have to be extended in significant ways. While the minimal model borrowed from refs 32−34 gave a decent account of most of the experimental data, it already was showing signs of breaking down for higher polyads. H_2O seems like a very good case for the next level of complexity since it has a very extensively cataloged absorption spectrum.

Acknowledgment. This work was supported by the U.S. Department of Energy Basic Energy Sciences program under Contract DE-FG02-05ER15634.

References and Notes

(1) Kellman, M. E.; Tyng, V. *Acc. Chem. Res.* **2007**, *243*, 40.
(2) Kellman, M. E. Algebraic Methods in Spectroscopy. *Annu. Rev. Phys. Chem.* **1995**, *46*, 395–421.
(3) Xiao, L.; Kellman, M. E. *J. Chem. Phys.* **1989**, *90*, 6086–6098.
(4) Li, Z.; Xiao, L.; Kellman, M. E. *J. Chem. Phys.* **1990**, *92*, 2251–2268.
(5) Xiao, L.; Kellman, M. E. *J. Chem. Phys.* **1990**, *93*, 5805–5820.
(6) Kellman, M. E.; Xiao, L. *J. Chem. Phys.* **1990**, *93*, 5821–5825.
(7) Svitak, J.; Li, Z.; Rose, J.; Kellman, M. E. *J. Chem. Phys.* **1995**, *102*, 4340–4354.
(8) Lu, Z.-M.; Kellman, M. E. *Chem. Phys. Lett.* **1995**, *247*, 195–202.
(9) Rose, J. P.; Kellman, M. E. *J. Chem. Phys.* **1996**, *105*, 7348–7363.
(10) Lu, Z.-M.; Kellman, M. E. *J. Chem. Phys.* **1997**, *107*, 1–15.
(11) Joyeux, M.; Sugny, D.; Tyng, V.; Kellman, M. E.; Ishikawa, H.; Field, R. W.; Beck, C.; Schinke, R. *J. Chem. Phys.* **2000**, *112*, 4162–4172.
(12) Rose, J. P.; Kellman, M. E. *J. Phys. Chem. A* **2000**, *104*, 10471–10481.
(13) Kellman, M. E.; Rose, J. P.; Tyng, V. *Eur. Phys. J. D* **2001**, *14*, 225–230.
(14) Svitak, J. F.; Tyng, V.; Kellman, M. E. *J. Phys. Chem. A* **2002**, *106*, 10797–10805.
(15) Tyng, V.; Kellman, M. E. *J. Phys. Chem. B* **2006**, *110*, 18859–18871.
(16) Tyng, V.; Kellman, M. E. *J. Chem. Phys.* **2007**, *127*, 041101.
(17) Tyng, V.; Kellman, M. E. *J. Chem. Phys.* **2008**, *130*, 144311.
(18) Chakraborty, A.; Kellman, M. E. *J. Chem. Phys.* **2008**, *129*, 171104.

(19) Zhou, C.; Xie, D.; Chen, R.; Yan, G.; Guo, H.; Tyng, V.; Kellman, M. E. *Spectrochim. Acta, Part A* **2002**, *58*, 727–746.
(20) Joyeux, M.; Farantos, S. C.; Schinke, R. *J. Phys. Chem. A* **2002**, *106*, 5407–5421.
(21) Bredenbeck, J.; Beck, C.; Schinke, R.; Koput, J.; Stamatiadis, S.; Farantos, S. C.; Joyeux, M. *J. Chem. Phys.* **2000**, *112*, 8855–8865.
(22) Jost, R.; Joyeux, M.; Skokov, S.; Bowman, J. *J. Chem. Phys.* **1999**, *111*, 6807–6820.
(23) Keshavamurthy, S.; Ezra, G. S. *J. Chem. Phys.* **1997**, *107*, 156–179.
(24) Jacobson, M. P.; O'Brien, J. P.; Silbey, R. J.; Field, R. W. *J. Chem. Phys.* **1998**, *109*, 121–133.
(25) Jacobson, M. P.; Jung, C.; Taylor, H. S.; Field, R. W. *J. Chem. Phys.* **1999**, *111*, 600–618.
(26) Jung, C.; Taylor, H. S.; Jacobson, M. P. *J. Phys. Chem. A* **2001**, *105*, 681–693.
(27) (a) McCoy, A. B.; Sibert, E. L., III. *J. Chem. Phys.* **1996**, *105*, 459–468. (b) Sibert, E. L., III; McCoy, A. B. *J. Chem. Phys.* **1996**, *105*, 469–478.
(28) Prosmiti, R.; Farantos, S. C. *J. Chem. Phys.* **1995**, *103*, 3299–3314.
(29) Prosmiti, R.; Farantos, S. C. *J. Chem. Phys.* **2003**, *118*, 8275–8280.
(30) Xu, D.; Guo, H.; Zou, S.; Bowman, J. M. *Chem. Phys. Lett.* **2003**, *377*, 582–588.
(31) Semparithi, A.; Keshavamurthy, S. *Chem. Phys. Lett.* **2004**, *395*, 327–334.
(32) Dübal, H.-R.; Quack, M. *J. Chem. Phys.* **1984**, *81*, 3779–3791.
(33) Baggott, J. E.; Chuang, M.-C.; Zare, R. N.; Dübal, H. R.; Quack, M. *J. Chem. Phys.* **1985**, *82*, 1186–1194.
(34) Lewerenz, M.; Quack, M. *J. Chem. Phys.* **1988**, *88*, 5408–5432.
(35) Cihla, Z.; Chedin, A. *J. Mol. Spectrosc.* **1971**, *40*, 337–355.

JP904038F